

# Encoding Integers and Rationals on Neuromorphic Computers using Virtual Neuron

Prasanna Date  
Oak Ridge National Laboratory  
Oak Ridge, Tennessee 37830  
Email: datepa@ornl.gov

Shruti Kulkarni  
Oak Ridge National Laboratory  
Oak Ridge, Tennessee 37830  
Email: kulkarnisr@ornl.gov

Aaron Young  
Oak Ridge National Laboratory  
Oak Ridge, Tennessee 37830  
Email: youngar@ornl.gov

Catherine Schuman  
University of Tennessee  
Knoxville, Tennessee 37996  
Email: cschuman@utk.edu

Thomas Potok  
Oak Ridge National Laboratory  
Oak Ridge, Tennessee 37830  
Email: potokte@ornl.gov

Jeffrey Vetter  
Oak Ridge National Laboratory  
Oak Ridge, Tennessee 37830  
Email: vetter@ornl.gov

**Abstract**—Neuromorphic computers perform computations by emulating the human brain, and use extremely low power. They are expected to be indispensable for energy-efficient computing in the future. While they are primarily used in spiking neural network-based machine learning applications, neuromorphic computers are known to be Turing-complete, and thus, capable of general-purpose computation. However, to fully realize their potential for general-purpose, energy-efficient computing, it is important to devise efficient mechanisms for encoding numbers. Current encoding approaches have limited applicability and may not be suitable for general-purpose computation. In this paper, we present the virtual neuron as an encoding mechanism for integers and rational numbers. We evaluate the performance of the virtual neuron on physical and simulated neuromorphic hardware and show that it can perform an addition operation using 23 nJ of energy on average using a mixed-signal memristor-based neuromorphic processor. We also demonstrate its utility by using it in some of the  $\mu$ -recursive functions, which are the building blocks of general-purpose computation.

## I. INTRODUCTION

Neuromorphic computers perform computations by emulating the human brain [1]. Akin to the human brain, they are extremely energy efficient in performing computations [2]. For instance, while CPUs and GPUs consume around 70 W and 250 W of power, a neuromorphic computer consumes around 65 mW of power, i.e. 4–5 orders of magnitude less power than CPUs and GPUs [3]. The structural and functional units of neuromorphic computation are neurons and synapses, which can be implemented on digital or analog hardware [4]. They impart critical characteristics to neuromorphic computing such as co-located processing and memory, event-driven computation, massively parallel operation and inherent scalability [5]. These characteristics are crucial for the energy efficiency of neuromorphic computers. For the purposes of this paper, we define neuromorphic computing as any computing paradigm (theoretical, simulated, or hardware) that performs computations by emulating the human brain, i.e., by using neurons and synapses, that communicate with binary-valued signals (also known as spikes).

Neuromorphic computing is primarily used in machine learning applications, almost exclusively leveraging spiking neural networks (SNN) [6]. In the recent years however, it has also been used in non-machine learning applications such as graph algorithms, boolean linear algebra and neuromorphic simulations [7]–[9]. Researchers have also shown that neuromorphic computing is Turing-complete, i.e. capable of general-purpose computation [10]. This ability to perform general-purpose computations and potentially use orders of magnitude less energy in doing so is why neuromorphic computing is poised to be an indispensable part of the energy-efficient computing landscape in the future. However, in order to realize a fully operational, general-purpose neuromorphic computer, we must address several limitations of today’s neuromorphic computing at the hardware and software level.

One of the biggest limitations of neuromorphic computing today is the inability to encode numbers efficiently [11]. While there are several studies on the performance of neural network models with low precision representation of parameters such as weights [12], these approximate representations are not suitable for general purpose computing. There exist several methods to encode numbers on neuromorphic computers [13]. However, their scope is restricted to the specific application for which they were designed and is not suitable for general-purpose computation. Furthermore, no good mechanism exists for encoding negative integers and positive and negative rational numbers exactly on neuromorphic computers. The ability to encode basic data types such as numbers, letters and symbols is vital for any computing platform. Efficient mechanisms for encoding rational numbers would significantly expand the scope of neuromorphic computing to new application areas such as non-SNN-based machine learning (regression, support vector machines etc.), wide range of graph and network problems, general-purpose computing applications, linear and non-linear optimization, simulation of physical systems and perhaps even finding good solutions to NP-complete problems. Working with rational numbers is

central to these application areas. Being able to encode rational numbers on a neuromorphic computer could enable us to address these problems in an energy-efficient manner.

Neuromorphic computers are seen as accelerators that can perform machine learning tasks using spiking neural networks. In order to perform any other operation (for example, arithmetic, logical, relational, etc.), we still resort to CPUs and GPUs because no good neuromorphic methods exist to perform these operations. To perform these operations, we have to transfer data from the neuromorphic computer to CPUs/GPUs, which incurs significant communication costs (more than 99% of the time is spent in communication) and is highly inefficient. Devising neuromorphic approaches for performing these non-machine learning operations would drastically reduce the cost of transferring data to and from the neuromorphic computer. This would enable performing all types of computation (machine learning as well as non-machine learning) efficiently on low power neuromorphic computers deployed on the edge.

To this extent, we present the virtual neuron for addressing the limitation of neuromorphic computers to encode numbers. This is the first step towards performing general-purpose computations on neuromorphic computers. To the best of our knowledge, the virtual neuron is the first encoding mechanism that can encode positive and negative integers and rational numbers on a neuromorphic computer. Specifically, our main contributions are:

- 1) We introduce the virtual neuron, which is made up of spiking neurons and synapses. It is a spatial encoding mechanism that leverages the binary representation of numbers to encode positive and negative integers and rational numbers. This is detailed in Section IV.
- 2) We implement the virtual neuron in the Neural Simulation Technology (NEST) simulator [14] and test its performance on 8, 16 and 32 bit rational numbers. We also discuss the computational complexity of the virtual neuron. This is outlined in Sections V and VI.
- 3) We analyze the performance of the virtual neuron on neuromorphic hardware by analyzing the run time using a digital neuromorphic hardware design, and we also estimate the energy usage of the virtual neuron on a mixed-signal memristor-based hardware design.
- 4) We demonstrate the usability of the virtual neuron by using it in five functions: constant function, successor function, predecessor function, multiply by  $-1$  function and  $N$ -neuron addition. This is covered in Section VII. Without the use of virtual neuron, implementing these functions on a neuromorphic computer would be extremely challenging.

## II. RELATED WORK

Neuromorphic computing was introduced by Carver Mead in the 1980s [15]. Since then, it is primarily used for SNN-based machine learning applications, including computer vision [16], natural language [17] and speech recognition [18]. These applications are mainly found in embedded systems,

edge computing and Internet of Things (IoT) settings as they have strict requirements for small size, weight and power [19]–[21]. Several on-chip as well as off-chip learning algorithms that leverage gradient-based as well as local learning rules have been suggested for training SNNs in neuromorphic applications [22]–[25]. Neuromorphic computing has also been used in neuroscience simulations [26]. These simulations span a wide range of neuron and synapse models, the most popular of which is the leaky-integrate-and-fire (LIF) neuron model [27]. Our virtual neuron will use spiking neurons that are of the LIF type as well. The latest additions to the arsenal of neuromorphic computing applications include graph algorithms [7], [28], [29], autonomous racing [30], epidemiological simulations [9], classifying supercomputer failures [31],  $\mu$ -recursive functions [10], and boolean matrix-vector multiplication [8]. With regards to designing neuromorphic algorithms, a theoretical framework for determining the computational complexity has also been proposed [32].

Most of the above applications are based on binary numbers and Boolean arithmetic. This is largely due to the spiking behavior of the neuron—the spikes can be interpreted as a 1, whereas lack of spike can be interpreted as a 0. This spiking behavior naturally lends itself to binary or Boolean operations. Leveraging this behavior, several mechanisms for encoding numbers (mainly positive integers) have been proposed in the literature. Choi et al. propose a neuromorphic implementation of hypercolumns, including mechanisms for encoding images [33]. Cohen et al. use neuromorphic methods to classify images that have been encoded as spikes [34]. Hejda et al. present a mechanism for encoding image pixels as rate-coded optical spike trains [35]. Sengupta and Roy encode neural and synaptic functionalities in electron spin as an efficient way to perform neuromorphic computation [36]. Yi et al. propose a field programmable gate array (FPGA) platform to be used as a spike time dependent encoder and dynamic reservoir in neuromorphic computers [37].

Iaroshenko and Sornborger propose neuromorphic mechanisms for encoding binary numbers, and use it for binary two's complement operations and binary matrix multiplication [38]. However, their approach uses numbers of neurons and synapses that are of the quadratic and cubic order respectively. Lawrence et al. perform neuromorphic matrix multiplication by using an intermediate transformation matrix for encoding that is flattened into a neural node [39]. Schuman et al. propose three ways of encoding positive integers on neuromorphic computers, which are in turn used in many different applications [13]. Zhao et al. develop a compact, low power, and robust spiking-time-dependent encoder, designed with a LIF neuron cluster and a chaotic circuit with ring oscillators [40]. Zhao et al. develop a method for representing data using spike time dependent encoding that efficiently maps a signal's amplitude to a spike time sequence representing the input data [41]. Zhao et al. propose an analog temporal encoder for making neuromorphic computing robust and energy efficient [42]. Wang et al., made use of radix encoding of spike to realize SNNs more efficiently and improve the speedup by

reducing the overall latency for machine learning applications [43]. Other efforts to realize basic computations on neuromorphic platforms leveraging the inherent structure and parameters of SNNs for logic operations such as AND, OR and XOR have been demonstrated in [44]. George et al., performed IEEE 754 compliant addition using SNNs by designing a system based on the Neural Engineering Framework (NEF) and implemented, simulated, and tested the design using Nengo [45]. This approach uses an ensemble of 300 neurons to represent each bit and the function of each component in the adder is approximated using NEF to determine the appropriate synapse weights. Dubey et al., extend this work to perform IEEE 754 compliant multiplication using the same encoding method and similar methodology of using NEF to approximate the functions of the multiplier sub-components [46].

Most of these encoding mechanisms have the ability to encode binary or Boolean numbers, with some being able to encode positive integers as well. These methods are designed with specific applications in mind such as image applications, and it is not clear if they can be used for general-purpose neuromorphic computation, where arithmetic operations need to be performed on positive and negative integers/rationals. Moreover, some of the encoding mechanisms such as binning tend to lose information by virtue of discretization. To the best of our knowledge, an efficient mechanism for encoding positive and negative rational numbers does not exist in the neuromorphic literature yet. We address this gap by proposing the virtual neuron. In our quest for general-purpose, energy-efficient neuromorphic computing, being able to encode rational numbers is a critical milestone.

### III. NEUROMORPHIC COMPUTING MODEL

Neuromorphic computing systems implement vastly different neuron and synapse models, and the precise model details depend on the specific hardware implementation. We leverage the neuromorphic computing model described in [10] and [32], which is based on the LIF neuron with two parameters (threshold,  $\nu$  and leak  $\lambda$ ), and two synapse parameters (weight,  $\omega$  and delay,  $\delta$ ).

### IV. THE VIRTUAL NEURON

Structurally, the virtual neuron is composed of a group of LIF neurons and synapses that are connected in a particular way. Functionally, the virtual neuron mimics the behavior of an artificial neuron with identity activation. The virtual neuron is an encoding mechanism as well as an adder. It performs the addition operation similar to a ripple carry adder. The rationale behind the encoding mechanism of the virtual neuron is rooted in the binary encoding of numbers. Figure 1 shows three ways of encoding four bit numbers on a neuromorphic computer. Notice that each neuron in the figure represents a bit. The synapse coming out of the neuron assigns a value to the binary spike of the neuron by multiplying it with its synaptic weight. By having powers of two as the synaptic weights, we can encode rational numbers using a group of neurons. For instance, the synapses coming out of the four neurons in Figure

1a have weights  $2^0$ ,  $2^1$ ,  $2^2$  and  $2^3$ . When the second and fourth neurons (from the bottom) spike, the result gets multiplied by 2 and 8 in the outgoing synapses respectively. This is interpreted as the number 10 under this encoding mechanism. Similarly, we can set the synaptic weights to be negative powers of two as shown in Figure 1b. This enables us to encode positive fractions as well. When the first and third neurons (from the bottom) spike as shown in the figure, the result is interpreted as a 0.625. Lastly, if the synaptic weights are set to negatives of positive and negative powers of two as shown in Figure 1c, we can encode negative rational numbers. When the three neurons spike in the figure, the output is interpreted as  $-3.5$ .

We now show how the virtual neuron can integrate the incoming signals and generate a rational number as output. For ease of explanation, we stick to the two-bit virtual neuron as shown in Figure 2. The two-bit virtual neuron takes as input two 2-bit numbers  $X$  and  $Y$ , shown in the figure as  $[x_1, x_0]$  (blue neurons) and  $[y_1, y_0]$  (yellow neurons) respectively. It then adds  $X$  and  $Y$  in the three groups of bit neurons, which are shown in red. We call them bit neurons because they are responsible for the bit-level operations in the circuit such as bitwise addition, propagating the carry bit etc. Finally, it produces a 3-bit number  $Z$  as output, shown in the figure as  $[z_2, z_1, z_0]$  (green neurons).

The default internal states of all neurons are set to  $-1$ . Furthermore, all neurons have a leak of 0, which means they reset to their default internal state instantaneously if they do not spike. The reset state (or reset voltage) of all neurons is set to  $-1$ , so that the internal state of all neurons will be reset to  $-1$  after they spike. The numbers on the neurons indicate their thresholds, for e.g., the top set of bit neurons (red neurons) have thresholds 0, 1 and 2 respectively. The synapse parameters are indicated in angular brackets on top or bottom of the synapses. The first parameter is the synaptic weight and the second parameter is the synaptic delay. If a group of synapses has the same parameters, it is indicated using a dotted arc. The synaptic delays are adjusted such that the bit operations of red neurons are synchronized and the output  $Z$  is produced at the same time.

We now go over the inner workings of the virtual neuron shown in Figure 2 by taking the example:  $[x_1, x_0] = [1, 1]$ , and  $[y_1, y_0] = [0, 1]$ . We start our analysis when the inputs  $X$  and  $Y$  have been received in the blue and yellow neurons—let us call this the zeroth time step. In the first time step, the bottom set of bit neurons in red receive an input of 1 along each of their incoming synapses. Thus, the total incoming signal at both these neurons is 2, which changes their internal state from  $-1$  to 1. As a result, both the bottom red neurons spike. Their spikes are sent along their outgoing synapses, which delay the signal for 3 time steps.

In the second time step, the middle group of bit neurons receive all of their inputs: 1 from the blue incoming neuron representing  $x_1$ , 0 from the yellow neuron representing  $y_1$  and 1 from the bit neuron with a threshold of 1 in the bottom group. Thus, sum of their incoming signals is 2 and their internal states reach a value of 1. As a result, neurons with thresholds 0

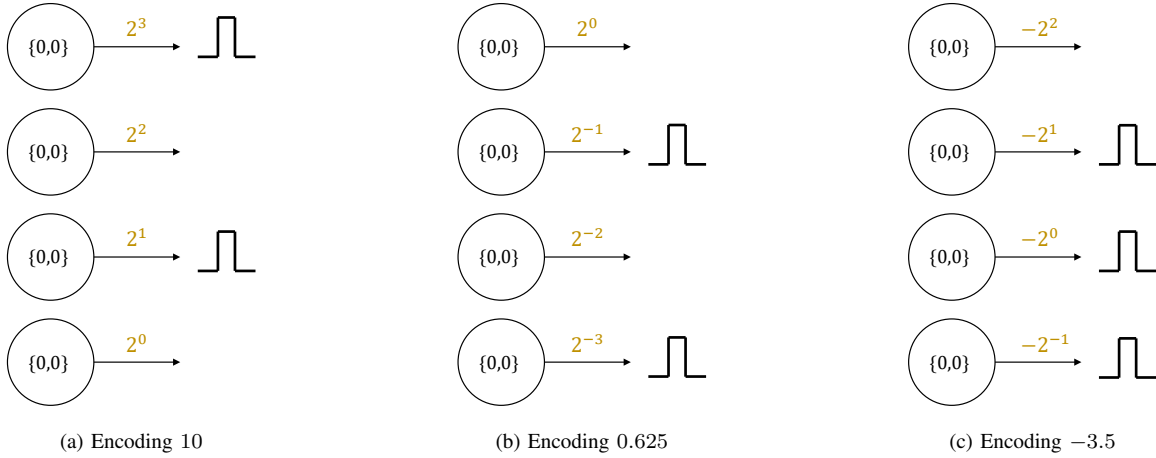


Fig. 1. Encoding mechanism of the virtual neuron. Numbers can be encoded by selecting appropriate synaptic weights. Here, we use four neurons to encode: (1a) positive integers; (1b) positive rationals; and, (1c) negative rationals. The four spiking neurons can encode four bits of information.

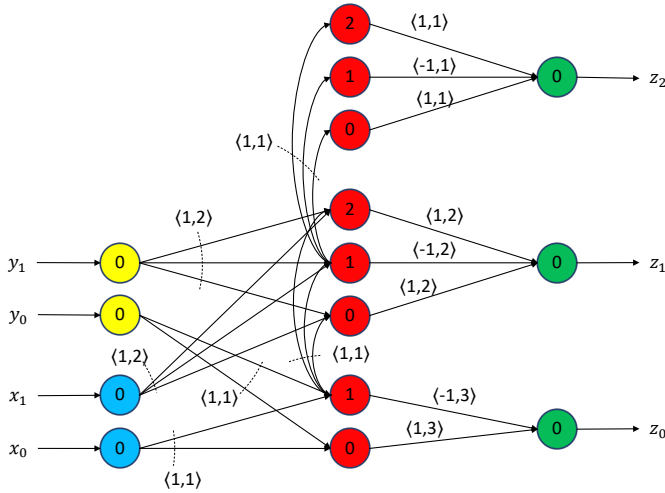


Fig. 2. Two-bit virtual neuron. Takes two 2-bit numbers as input on the left:  $X$  and  $Y$ , represented as  $x_1, x_0$  and  $y_1, y_0$  respectively. Adds the two numbers and generates their sum on the right. The sum of two 2-bit numbers can at most be a 3-bit number.

and 1 in the middle group of bit neurons spike, whereas the one with threshold 2 does not spike. The spikes from the middle red neurons with thresholds 0 and 1 are sent to the green output neuron representing  $z_1$  along their outgoing synapses, which stall for 2 time steps.

In the third time step, the three bit neurons in the top group of red neurons receive an input of 1 along each of their incoming synapses. As a result, their internal states are incremented by 1 to the value of 0. The neuron with 0 threshold spikes as a result and sends its spike along its outgoing synapse to the green neuron representing  $z_2$ .

In the fourth time step, the green neurons representing  $z_0, z_1$  and  $z_2$  receive their inputs.  $z_0$  receives a 1 and  $-1$  from the bit neurons with the thresholds 0 and 1 respectively in the bottom group of red neurons. Its total input is thus  $1 - 1 = 0$ , which keeps its internal state at  $-1$ , and it does not spike. Similar

operations happen at the green neuron representing  $z_1$ . It too does not spike. The green neuron representing  $z_2$  receives a signal of 1 from the bit neuron with the threshold of 0 in the top red set. As a result, its internal state is incremented by 1 to the value of 0, and it spikes.

The net output  $[z_2, z_1, z_0]$  from the circuit is  $[1, 0, 0]$ , which can be interpreted as a 4 in binary. Given that our inputs were  $[x_1, x_0] = [1, 1]$ , and  $[y_1, y_0] = [0, 1]$ , i.e.,  $X = 3$ , and  $Y = 1$ , we have received the correct output of 4 from the virtual neuron circuit. While we restricted ourselves to 2-bit positive integers in this example, we show in the subsequent subsections that similar circuits can be used to encode and add two rational numbers in the virtual neuron and generate a rational number as output. Finally, note that we did not use powers of two in the synapses inside of the virtual neuron. Depending on the application, powers of two as synaptic weights may be used on the incoming or outgoing synapses for a given virtual neuron.

In the following subsections, we present virtual neuron circuits that have higher precision. We let  $P_+$  and  $P_-$  denote the number of bits used to represent positive and negative numbers respectively. We call them positive precision and negative precision respectively. In general, the positive precision  $P_+$  will be distributed among bits used to represent positive integers ( $2^0, 2^1, 2^2, \dots$ ) and positive fractionals ( $2^{-1}, 2^{-2}, 2^{-3}, \dots$ ). Similarly, the negative precision  $P_-$  will be distributed among bits used to represent negative integers ( $-2^0, -2^1, -2^2, \dots$ ) and negative fractionals ( $-2^{-1}, -2^{-2}, -2^{-3}, \dots$ ).

We now describe the connections for a virtual neuron with arbitrary precision. Each input neuron has both threshold and leak as zero. Each input  $x_i$  and  $y_i$  is connected to the set of bit neurons corresponding to bit  $i$ . In the case of bit 0 there are two such bit neurons, while for every other bit, there are three neurons per bit shown in red. The synaptic weights of all these connections are unity and their delays are  $i + 1$ . Each set of bit neurons has neurons with thresholds of zero and one. All bit neurons except the zero bit have a neuron with

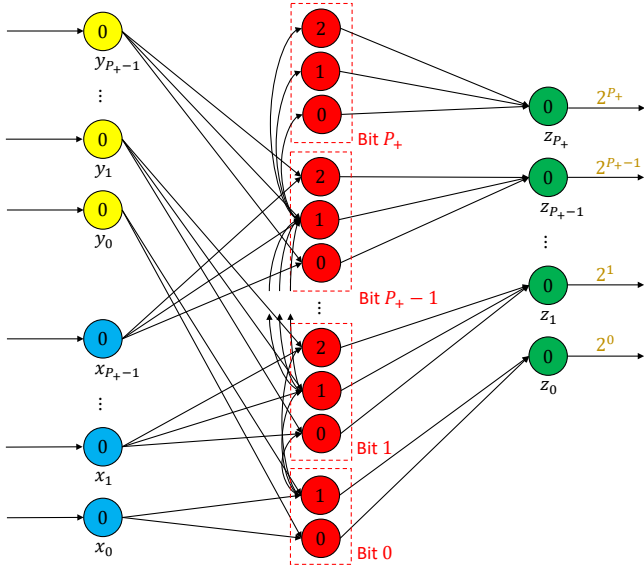


Fig. 3.  $P_+$  bit virtual neuron for encoding positive integers. Synapse parameters are omitted for brevity. Actual synapse parameters are assumed to be similar to the circuit shown in Figure 2.

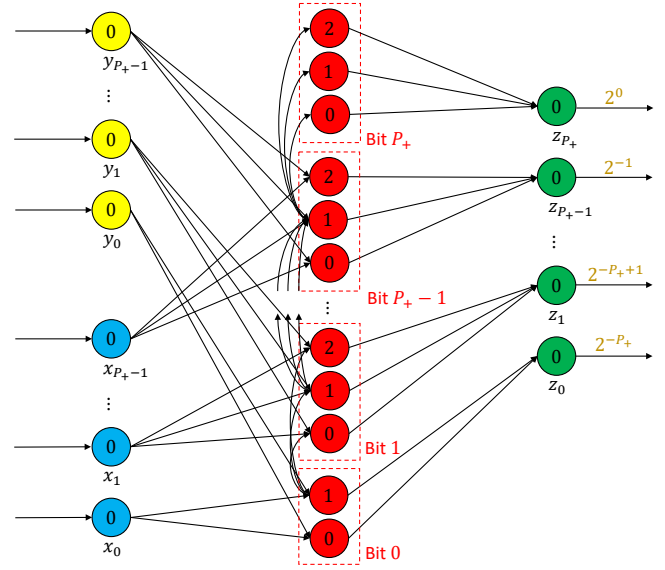


Fig. 4.  $P_+$  bit virtual neuron for encoding positive fractionals. Synapse parameters are omitted for brevity. Actual synapse parameters are assumed to be similar to the circuit shown in Figure 2.

a threshold of two as well. The neuron with a threshold of one in the set of neurons representing bit  $i$  is connected to all neurons in the  $(i + 1)$ -th set. This neuron is responsible for the propagating the carry bit to the next set of bit neurons. It spikes only when there is a carry operation to be performed at the  $i$ -th bit. The carry synapses have both weights and delays as unity. The bit neurons of the  $i$ -th bit are connected to the  $i$ -th output neuron. The synaptic weights for the bit neurons having thresholds of zero and two are 1, while those for the bit neurons having threshold of one are  $-1$ . The  $-1$  weight is seen as an inhibitory connection that cancels the signal coming from the neuron with threshold zero in the same bit set. The delays on the synapses going from  $i$ -th bit set to the  $i$ -th output neuron are set to  $\max\{P_+, P_-\} - i + 1$ . This delay ensures that all output neurons spike at the same time.

#### A. Positive Integers

Figure 3 shows the virtual neuron circuit that takes two  $P_+$  bit numbers  $X$  and  $Y$  as inputs, shown as blue and yellow neurons respectively. The bit-level addition and carry operations are performed by the bit neurons shown in red. There are  $P_+ + 1$  groups of these bit neurons. Finally, the output of the virtual neuron  $Z$  has  $P_+ + 1$  bit precision, and is shown by the green output neurons. In the figure, we omit synapse parameters for brevity. Notice that the synaptic weights on the outgoing synapses are positive powers of 2.

#### B. Positive Fractionals

Figure 4 shows the  $P_+$  bit virtual neuron for encoding positive fractionals. The circuit is almost identical to Figure 3. The only difference is in the synaptic weights of the outgoing synapses. In this case, these synapses have negative powers of two, i.e.,  $2^0, 2^{-1}, 2^{-2}, 2^{-3}, \dots$  as their weights.

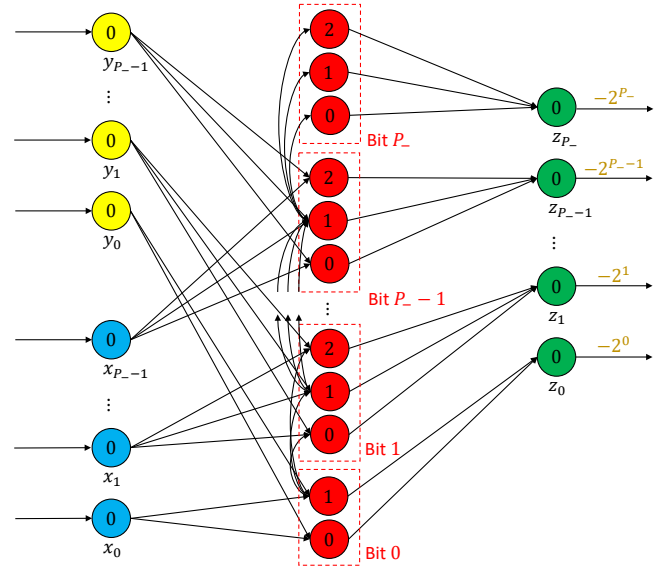


Fig. 5.  $P_-$  bit virtual neuron for encoding negative integers. Synapse parameters are omitted for brevity. Actual synapse parameters are assumed to be similar to the circuit shown in Figure 2.

#### C. Negative Integers

Figure 5 shows the virtual neuron circuit for encoding negative integers. It takes two  $P_-$  bit numbers  $X$  and  $Y$  as inputs. After standard virtual neuron operations, a  $P_- + 1$  bit number  $Z$  is produced as the output. In this case, these weights are negatives of positive powers of two, i.e.,  $-2^0, -2^1, -2^2, \dots$

#### D. Negative Fractionals

Figure 6 shows the  $P_-$  bit virtual neuron circuit for encoding negative fractionals. This circuit is identical to Figure 5,

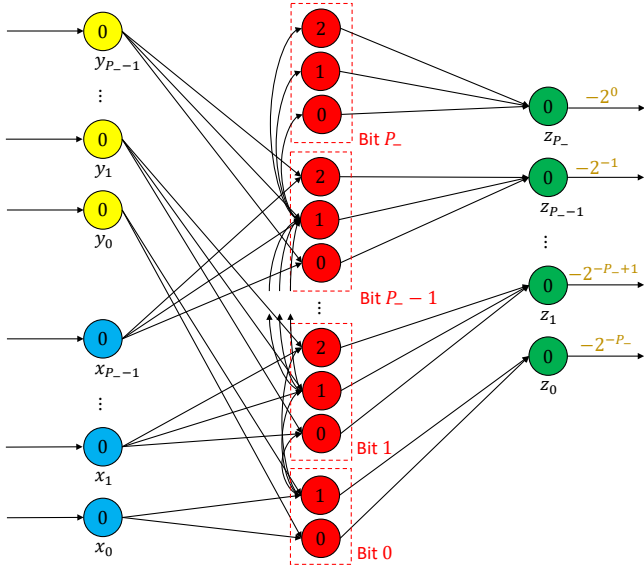


Fig. 6.  $P_-$  bit virtual neuron for encoding negative fractionals. Synapse parameters are omitted for brevity. Actual synapse parameters are assumed to be similar to the circuit shown in Figure 2.

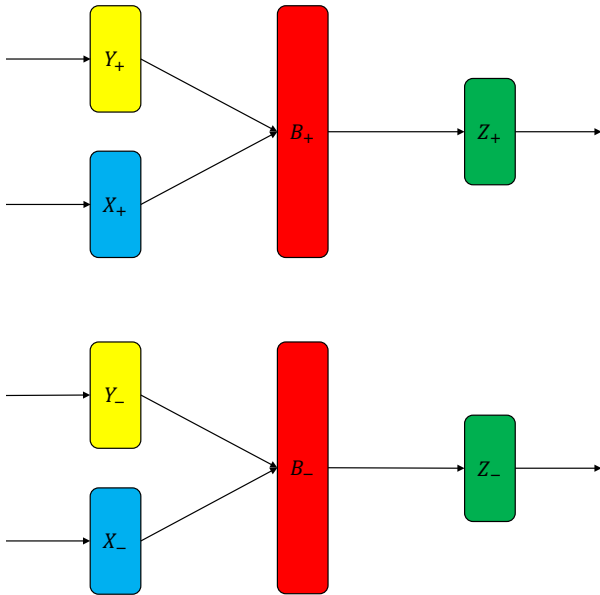


Fig. 7. Encoding  $P_+$  bit positive rationals and  $P_-$  bit negative rationals using virtual neuron.

except the outgoing synapses have weights that are negatives of negative powers of two, i.e.  $-2^0, -2^{-1}, -2^{-2}, \dots$

### E. Positive and Negative Rational Numbers

In this case, the virtual neuron operates on two  $P_+ + P_-$  bit rational numbers  $X$  and  $Y$  as inputs. These are shown in blue and yellow rectangles, which denote aggregation of respective neurons. The positive precision  $P_+$  is split between the positive integers and positive fractionals. Similarly, negative

TABLE I  
NEURONS, SYNAPSES AND TIME TAKEN WITH INCREASING PRECISION.

Number of bits of positive precision ( $P_+$ )	Number of neurons	Number of synapses	Time steps for virtual neuron operations
1	9	12	3
2	15	24	4
4	27	48	6
8	51	96	10
16	99	192	18
32	195	384	34
64	387	768	66
128	771	1536	130

TABLE II  
COMPARING VIRTUAL NEURON TO OTHER NEUROMORPHIC ENCODING MECHANISMS FOR REPRESENTING TWO  $N$ -BIT NUMBERS EXACTLY.

Metrics	Binning [13]	Rate [13]	Time [13]	Virtual Neuron	IEEE-754 [45], [46]
Time Required (big- $\mathcal{O}$ )	$\mathcal{O}(1)$	$\mathcal{O}(2^N)$	$\mathcal{O}(2^N)$	$\mathcal{O}(1)$	$\mathcal{O}(1)$
# Neurons (big- $\mathcal{O}$ )	$\mathcal{O}(2^N)$	$\mathcal{O}(1)$	$\mathcal{O}(1)$	$\mathcal{O}(N)$	Ensembles of $N$ neurons with dimension and radius properties <sup>1</sup> $\mathcal{O}(N)^2$
Accuracy	100%	100%	100%	100%	>90% at 500 Neurons per bit. Encoded error at 0 with >300 Neurons per bit.
Energy Efficiency (# of spikes in the worst case)	$\mathcal{O}(1)$ spikes	$\mathcal{O}(2^N)$ spikes	$\mathcal{O}(1)$ spikes	$\mathcal{O}(N)$ spikes; $N$ spikes	Energy results unpublished
Energy Efficiency (# spikes in the average case)	$\mathcal{O}(1)$ spikes	$\mathcal{O}(2^N)$ spikes	$\mathcal{O}(1)$ spikes	$\mathcal{O}(N)$ spikes; $N/2$ spikes	Energy results unpublished

<sup>1</sup>Dimension refers to the number of values represented by the ensemble. (For a scalar quantity this is 1). Radius defines the range of values that can be represented by the ensemble. For the cited work dimension is 1 and radius is set to 2.

<sup>2</sup>Authors only looked at IEEE floating point, so how the representation scales with numerical precision is unclear.

precision is split between the negative integers and negative fractionals. Notice that the positive part of the circuit (upper half) is completely independent from the negative part of the circuit (lower half).

### F. Computational Complexity

For  $P_+$  bit positive operations, we use  $\mathcal{O}(P_+)$  neurons and synapses, and perform the virtual neuron operations in  $\mathcal{O}(P_+)$  time steps. Similarly, for  $P_-$  bit negative operations, we use  $\mathcal{O}(P_-)$  neurons and synapses, and perform the virtual neuron operations in  $\mathcal{O}(P_-)$  time steps. All in all, we use  $\mathcal{O}(P_+ + P_-)$  neurons and synapses, and consume  $\mathcal{O}(\max\{P_+, P_-\})$  time steps for the virtual neuron operations.

We validate these space and time complexities empirically for positive operations by increasing  $P_+$ . The results of this analysis apply to negative operations as well. We increase the positive precision from 1, 2, 4, ..., 128 and count the number of neurons, synapses and time steps in each case. The

TABLE III  
COMPARING VIRTUAL NEURON TO OTHER NEUROMORPHIC ENCODING MECHANISMS FOR ADDING TWO N-BIT NUMBERS.

Metrics	Binning [13]	Rate Encoding [13]	Virtual Neuron	IEEE 754 [45]
Time to solution	$\mathcal{O}(1)$	$\mathcal{O}(2^N)$	$\mathcal{O}(N)$	Constant
# Neurons	$\mathcal{O}(2^N)$	$\mathcal{O}(1)$	$\mathcal{O}(N)$	3075
# Synapses	$\mathcal{O}(2^N)$	$\mathcal{O}(1)$	$\mathcal{O}(N)$	N/A
Energy Efficiency (# spikes in the worst case)	$\mathcal{O}(2^N)$	$\mathcal{O}(2^N)$	$\mathcal{O}(N)$	N/A
Energy Efficiency (# spikes in the average case)	$\mathcal{O}(2^N)$	$\mathcal{O}(2^N)$	$\mathcal{O}(N)$ ; N/2	N/A
Accuracy	100% <sup>1</sup>	Depends on model type	100%	100% with 300 Neurons per bit

<sup>1</sup>Accuracy is bound by the synapse weight and accumulation accuracy.

numerical results are presented in Table I. From the table, we can conclude that we use  $6P_+ + 3$  neurons,  $12P_+$  synapses and  $P_+ + 2$  time steps for virtual neuron operations.

We can extend these time complexities to negative operations to conclude that they would require  $6P_- + 3$  neurons,  $12P_-$  synapses and  $P_- + 2$  time steps. This validates the space complexity as needing  $\mathcal{O}(P_+ + P_-)$  neurons and synapses. Since the positive and negative operations happen parallelly, the overall time complexity of the circuit would stem from the larger of  $P_+$  and  $P_-$ . So, the overall time complexity is validated as  $\mathcal{O}(\max\{P_+, P_-\})$ .

Lastly, in computing the above space and time complexities, our inherent assumption is that the positive and negative precisions are variable. However, we envision using the virtual neuron in settings where a neuromorphic computer has a fixed predetermined positive and negative precision. This is similar to how the precision on our laptops and desktops is fixed to 32, 64 or 128 bits. In such a scenario,  $P_+$  and  $P_-$  can be treated as constants. Thus, the resulting space and time complexities for virtual neuron would all be  $\mathcal{O}(1)$ .

Table II presents a comparison of different neuromorphic encoding approaches in the literature with our approach using the virtual neuron. Since a neuromorphic computer consumes energy that is proportional to the number of spikes, we use the number of spikes in the worst and average case as an estimate for the energy usage of different neuromorphic approaches. It can be seen that across different comparison metrics such as network size, or number of spikes, the virtual neuron scales linearly with the bit-precision  $N$ , while giving the exact representation of the input number. Other approaches take either exponential space (Binning), or exponential time (Rate Encoding), or are unable to represent rational numbers exactly (IEEE 754). Table III presents the comparison of computational complexity for performing addition with two N-bit numbers under different neuromorphic encoding schemes. Here we do not include temporal encoding scheme because under such a simple approach, binary spikes occurring at different time instances cannot be added in an exact manner

by spiking neurons. While the virtual neuron can perform the addition operation in linear time steps and using linear number of neurons, synapses and energy (as estimated by the spiking efficiency), other approaches use either exponential time or exponential space or consume exponential amount of energy for their operations.

## V. IMPLEMENTATION DETAILS

We implemented the virtual neuron in Python using the NEST simulator. The hardware on which the simulations were run was a MacBook Pro having a 2.3 GHz Quad-Core Intel Core i7 processor and 32 GB 3733 MHz LPDDR4X memory. We wrote a `VirtualNeuron` class, whose constructor took a list-like object of length 4 as the precision vector. The elements of this vector corresponded to number of bits for positive integers, positive fractionals, negative integers and negative fractionals. We then computed the positive precision as the sum of the first two elements of the precision vector, and the negative precision as the sum of the third and fourth elements of the precision vector.

We then created all the neurons and set their parameters correctly. We used the `iaf_psc_delta` neuron model. All neurons had an internal state of  $-1.0$ . In NEST, the internal state corresponds to the voltage of the membrane potential (`V_m`) parameter. All neurons had a leak of  $10^{-6}$ , which is a good approximation to 0 leak that we require in our circuits. In NEST, the leak corresponds to the `tau_m` neuron parameter. All neurons except the bit neurons (red neurons) had a neuron threshold of 0. The group of bit neurons corresponding to the least significant bit in both the positive and negative parts of the circuit had only two neurons with thresholds 0 and 1. All other groups of bit neurons had three neurons with thresholds 0, 1 and 2 respectively. There were  $P_+$  ( $P_-$ ) such groups in the positive (negative) part of the circuit, making a total of  $P_+ + 1$  ( $P_- + 1$ ) groups of bit neurons, corresponding to the  $P_+ + 1$  ( $P_- + 1$ ) output bits in the positive (negative) parts of the circuit.

After the neurons were created, we setup the synapses. Firstly, synapses between the positive (negative) incoming neurons and positive (negative) bit neurons were created. These synapses had synaptic weights as 1.0 and synaptic delays as  $i+1$ , where  $i$  ranges from 0 to  $P_+$  ( $P_-$ ). Secondly, we setup the carry synapses between the consecutive groups of positive (negative) bit neuron groups. The carry synapses go from the bit neuron having a threshold of 1 in the  $i^{\text{th}}$  group to all neurons in the  $(i+1)^{\text{th}}$  group, where  $i$  goes from 0 to  $P_+$  ( $P_-$ ). The carry synapses had both weights and delays as 1.0. Finally, we setup synapses from groups of positive (negative) bit neurons to their corresponding outgoing neurons. The synapses coming from bit neurons with thresholds 0 and 2 had weights 1.0, whereas those coming from bit neurons with thresholds 1 had weights of  $-1.0$ . Furthermore, these synapses in the positive (negative) part of the circuit had delays given by  $\max\{P_+, P_-\} - i + 1$  for  $i$  ranging from 0 to  $P_+$  ( $P_-$ ). We also wrote a function `connect_virtual_neurons(A, B, C)`, that connects three virtual neurons A, B and C such

that A and B serve as inputs to C. The weights and delays on these synapses were all 1.0.

## VI. TESTING RESULTS

We tested our implementation of the virtual neuron on 8, 16 and 32 bit rational numbers. The precision vectors fed to the class constructors in each of these cases were  $[2, 2, 2, 2]$ ,  $[4, 4, 4, 4]$ , and  $[8, 8, 8, 8]$  respectively. We connected three virtual neurons using the `connect_virtual_neurons` function described above. Next, we generated two numbers within the appropriate precision by generating spikes through the `spike_generator` in NEST, and then sent these spikes to the input virtual neurons A and B. We let the simulation run for a time long enough so that we receive an output from virtual neuron C. Lastly, we checked if output received from C was indeed the sum of numbers sent to A and B.

### A. 8 Bit Virtual Neuron

For the 8 bit case, we tested all permutations of the input numbers—a total of 65,536 cases. A randomly selected sample of results are shown in Table IV. It can be seen clearly that  $X_+ + Y_+ = Z_+$ , and  $X_- + Y_- = Z_-$  for all rows. The binary representations of  $X$  and  $Y$  were fed to the input neurons and the binary representation of  $Z$  was received as the output of the circuit.

### B. 16 Bit Virtual Neuron

The results from the 16 bit testing are shown in Table V. In this case, we tested 100,000 permutations of inputs, generated uniformly at random. A snippet of the results are shown in Table V. One can infer that the virtual neuron is mimicking an artificial neuron having an identity activation function, and that we are able to encode positive and negative rational numbers on a neuromorphic computer using this approach.

### C. 32 Bit Virtual Neuron

For the 32 bit case, we generated 100,000 permutations of inputs uniformly at random. Five randomly selected permutations are presented in Table VI. Once again, it can be concluded that the virtual neuron is successfully able to encode and add rational numbers on neuromorphic computers and scales linearly with the positive and negative precisions.

### D. Caspian and Hardware Testing

We also implemented and tested the 16-bit virtual neuron using the Caspian simulator and  $\mu$ Caspian digital FPGA hardware [47]. Since  $\mu$ Caspian does not implement synaptic delay, but instead implements axonal delay, the virtual neuron implementation was adjusted to use axonal delay instead of synaptic delay. The rest of the structure is the same as the NEST virtual neuron implementation, this means that the neuron and synapse counts and network time steps to solution are the same as in the NEST implementation.

$\mu$ Caspian is a digital neuromorphic processor implementation using an FPGA, the processor is event-based and processes all the spikes that occur at one time step before moving to the next time step. Time multiplexing of neurons is

used to reduce the size of the design.  $\mu$ Caspian is intentionally designed targeting the small and low-power iCE40 UP5k FPGA. Because of this,  $\mu$ Caspian only supports up to 256 neurons and 4096 synapses. This is enough to support up to a 32-bit virtual neuron adder; however, to include room for the input and output neurons, we tested with the 16-bit virtual neuron. Since  $\mu$ Caspian run time depends on activity, we ran 1,000 permutations of inputs selected uniformly at random on the  $\mu$ Caspian simulator and hardware, and monitored the total number of spikes and the number of cycles used by the processor.  $\mu$ Caspian has a behaviourally accurate software simulator and the hardware design can be emulated in Verilator or run on the FPGA. In this case we used the UPduino V3 as the FPGA board.

Over the 1,000 runs, the simulator reported 73,159 total spikes for an average of 73 spikes per test case. Using Verilator, the 1,000 test cases finished in  $\sim 5,000,000$  clock cycles. Where  $\sim 7,000$  cycles were used to load the virtual neuron network and  $\sim 5,000$  cycles are used per test case. Since the processor runs at 25 MHz, the total runtime without the overheads from communication with the host computer is  $\sim 0.21$ s for all the test cases. When we ran the test using the UPduino FPGA, the total time was  $\sim 400$ s. One main culprit for this slowdown is the 3 MBaud UART connection between the host and the FPGA. While running on hardware, over 99.9% of the execution time was spent in overhead and communication. This result highlights the great benefit of using the virtual neuron to perform addition on the SNN system instead of moving the data to a separate processor to perform the addition. The results from the hardware evaluation are tabulated in Table VII and a summary of the  $\mu$ Caspian processor cycles from the experiment are in Table VIII.

### E. mrDANNA Power Estimate

With neuromorphic application-specific integrated circuits, the power required for a particular network execution can be estimated based on the energy required for active and idle neurons and synapses for the duration of the execution. To estimate the power of the virtual neuron design, we used the same method and energy-per-spike values as reported in [48] for the mrDANNA mixed-signal memristor-based neuromorphic processor. Using the same number of spikes, neurons, and synapses as reported in the  $\mu$ Caspian simulation, we estimate that a mrDANNA hardware implementation would use  $\sim 23$  nJ for the average test case run and around  $\sim 23$  mW for continuous operation.

## VII. APPLICATIONS

In this section, we look at five functions where virtual neuron is used: constant function, successor function, predecessor function, multiply by  $-1$  function, and  $N$ -neuron addition.

### A. Constant Function

For a natural number  $x$ , the constant function returns a constant natural number  $k$ . It is defined as:

$$C_k(x) := k \quad (1)$$

TABLE IV

TESTING VIRTUAL NEURON ON 8-BIT RATIONAL NUMBERS. PRECISION IS [2, 2, 2, 2] FOR POSITIVE INTEGER, POSITIVE FRACTION, NEGATIVE INTEGER AND NEGATIVE FRACTION RESPECTIVELY.

$X_+$		$X_-$		$Y_+$		$Y_-$		$Z_+$		$Z_-$	
Decimal	Binary										
0.75	0011	-2.75	1011	1.0	0100	-2.5	1010	1.75	00111	-5.25	10101
2.5	1010	-3.75	1111	1.75	0111	-0.25	0001	4.25	10001	-4.0	10000
0.25	0001	-2.75	1011	2.75	1011	0.0	0000	3.0	01100	-2.75	01011
3.5	1110	-2.5	1010	3.5	1110	-0.25	0001	7.0	11100	-2.75	01011
3.0	1100	0.0	0000	3.25	1101	-1.0	0100	6.25	11001	-1.0	00100

TABLE V

TESTING VIRTUAL NEURON ON 16-BIT RATIONAL NUMBERS. PRECISION IS [4, 4, 4, 4] FOR POSITIVE INTEGER, POSITIVE FRACTION, NEGATIVE INTEGER AND NEGATIVE FRACTION RESPECTIVELY.

$X_+$		$X_-$		$Y_+$		$Y_-$		$Z_+$		$Z_-$	
Decimal	Binary	Decimal	Binary	Decimal	Binary	Decimal	Binary	Decimal	Binary	Decimal	Binary
2.5625	00101001	-11.375	10110110	13.3125	11010101	-6.75	01101100	15.875	011111110	-18.125	100100010
2.3125	00100101	-13.9375	11011111	11.375	10110110	-9.3125	10010101	13.6875	011011011	-23.25	101110100
15.875	11111110	-2.9375	00101111	1.5625	00011001	-4.6875	10001011	17.4375	100010111	-7.625	001111010
8.625	10001010	-10.1875	10100011	8.9375	10001111	-1.625	00011010	17.5625	100011001	-11.8125	010111101
14.6875	11101011	-10.625	10101010	11.625	10111010	-11.875	10111110	26.3125	110100101	-22.5	101101000

TABLE VI

TESTING VIRTUAL NEURON ON 32-BIT RATIONAL NUMBERS. PRECISION IS [8, 8, 8, 8] FOR POSITIVE INTEGER, POSITIVE FRACTION, NEGATIVE INTEGER AND NEGATIVE FRACTION RESPECTIVELY.

$X_+$	$X_-$	$Y_+$	$Y_-$	$Z_+$	$Z_-$
212.56640625	-203.421875	218.7265625	-98.91796875	431.29296875	-302.33984375
1.375	-4.36328125	184.94921875	-92.73046875	186.32421875	-97.09375
254.3359375	-134.390625	48.87109375	-211.43359375	303.20703125	-345.82421875
44.203125	-231.0703125	177.1171875	-207.06640625	221.3203125	-438.13671875
143.6171875	-8.1171875	214.41796875	-224.01953125	358.03515625	-232.13671875

TABLE VII  
SUMMARY OF HARDWARE EVALUATION

Method	Execution Time of Processor	Wall Time of Evaluation	Power
$\mu$ Caspian Hardware	0.21 s	400 s	
$\mu$ Caspian Simulator	N/A	747 ms	
mrDANNA	1 $\mu$ s @ 20MHz	N/A	23.04 mW

TABLE VIII  
 $\mu$ CASPIAN CYCLES SUMMARY

Entire Test			
Clock Cycles	5,000,000		
Total Time		0.21 s	
Per Test Average		0.21 ms	
Single Test Time		Network Load Time	
Clock Cycles	5,000	Clock Cycles	7,000
Time	0.21 ms	Time	0.29 ms

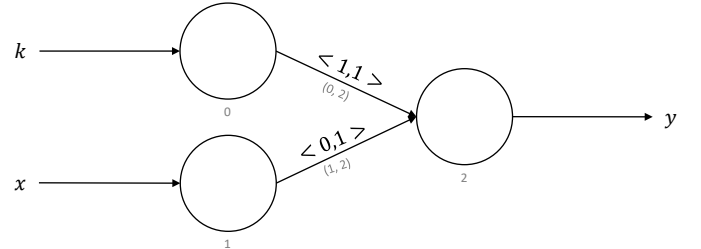


Fig. 8. Neuromorphic circuit for constant function

Figure 8 shows the neuromorphic circuit that computes the constant function. It has been adapted from [10] to work with the virtual neuron. Each neuron in this circuit is a virtual neuron. Inputs  $k$  and  $x$  are fed to the input neurons 0 and 1, and the output is produced at neuron 2. Synapses going from neuron 0 to neuron 2 have weights of 1, while those going from neuron 1 to neuron 2 have weights of 0. The constant function is one of the  $\mu$ -recursive functions.  $\mu$ -recursion is a model of computation that is equivalent to the

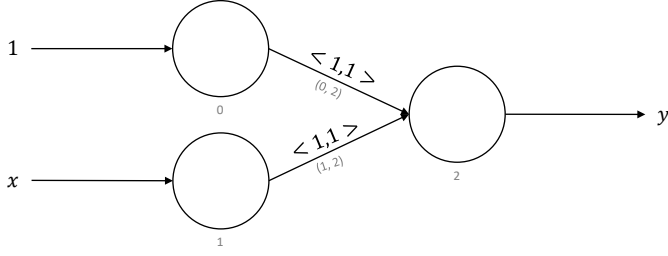


Fig. 9. Neuromorphic circuit for successor function

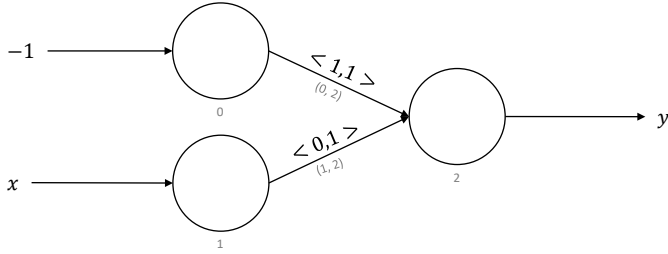


Fig. 10. Neuromorphic circuit for predecessor function

Turing machine. In order to prove that a computing platform is Turing-complete, it suffices to prove that it can execute all the  $\mu$ -recursive functions. In that light, being able to implement the constant function is a step towards empirically showing that neuromorphic computing is Turing-complete. We implemented the constant function circuit in NEST and tested it with 16 bit natural numbers. We were able to accurately execute the constant function using virtual neurons.

### B. Successor Function

For a natural number  $x$ , the successor function returns  $x+1$ . The successor of 0 is defined as 1. The successor function is defined as:

$$S(x) := x + 1 \quad (2)$$

Figure 9 shows the successor function. It too has been adapted from [10] and is another  $\mu$ -recursive function. It is similar to the constant function with a couple of differences. Neuron 0 is fed an input of 1 and synapse  $(1, 2)$  has a weight of 1. We implemented the successor function using three virtual neurons and tested it on 16-bit numbers. Our implementation was able to execute the successor function successfully.

### C. Predecessor Function

For a natural number  $x$ , the predecessor function returns  $x - 1$ . The predecessor function is defined as:

$$S(x) := x - 1 \quad (3)$$

Figure 10 shows the predecessor function. It is similar to the successor function with just one change. We feed an input

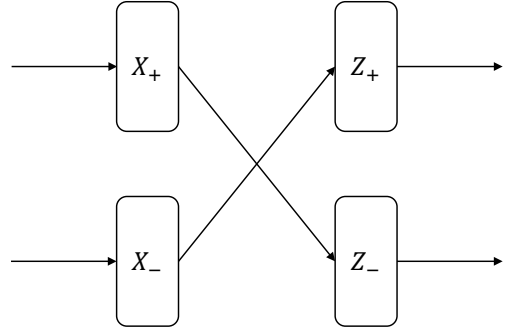


Fig. 11. Neuromorphic circuit to multiply a number by  $-1$ .

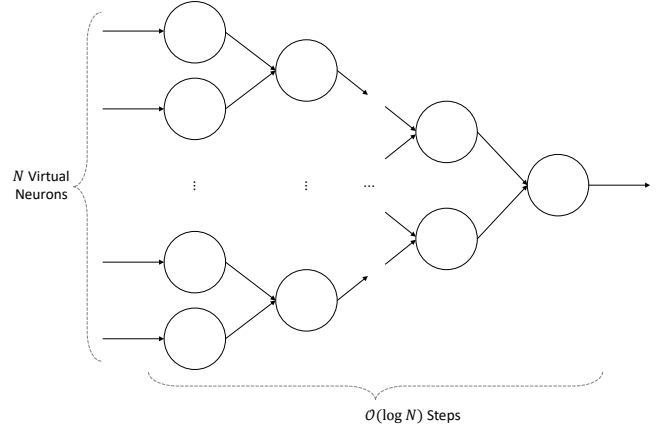


Fig. 12. Neuromorphic circuit to add  $N$  virtual neurons.

of  $-1$  to neuron 0 as opposed to 1. We implemented the predecessor function using three virtual neurons and tested it on 16 bit numbers. We were able to execute the predecessor function successfully using three virtual neurons in NEST.

### D. Multiply by -1

For a rational number  $x$  this function returns  $-x$ . Figure 11 shows the multiply by  $-1$  function. It takes a rational number encoded in virtual neuron  $X$ . In the figure, we use  $X_+$  to denote the positive part of  $X$  and  $X_-$  to denote negative parts of  $X$ . In this function, we assume that the number of positive and negative precision bits are equal. Under this assumption, we simply swap the positive and negative parts of  $X$  to return a number  $Z$  encoded as a virtual neuron. Since  $Z_+$  equals  $X_-$  and  $Z_-$  equals  $X_+$ , this function returns the negative of a number fed as the input. We implemented this function on 16 bit numbers and found that our virtual neuron-based implementation was able to execute the function successfully.

### E. N-Neuron Addition

The last application of virtual neuron that we want to highlight is the  $N$ -neuron addition. The figure for this application is shown in Figure 12, where we would like to add  $N$  virtual neurons given as inputs. The addition is performed

by successfully connecting pairs of input virtual neurons to a layer of virtual neurons, which in turn serve as inputs to the next layer. This method uses  $\mathcal{O}(N)$  virtual neurons and synapses and runs in  $\mathcal{O}(\log N)$  time steps. We implemented the  $N$ -neuron addition circuit in NEST and tested it on 16 bit numbers. This implementation was successfully able to add  $N$  virtual neurons in  $\mathcal{O}(\log N)$  time.

### VIII. DISCUSSION

In this paper, we proposed the virtual neuron as a mechanism for encoding as well as adding positive and negative rational numbers. Our work is a stepping stone towards a broader class of neuromorphic computing algorithms, that would enable us to perform general-purpose computations on neuromorphic computers. In this paper, we also measured the time, space, and energy required for virtual neuron operations and showed that it takes around 23 mW of power. In addition to a low operational power, there will be great savings in performing the operation withing the spiking array, without the need to spend energy sending the data to an external processor to perform the operation. Although it is out of the scope of this paper, the virtual neuron is a vital component to enabling composing of sub-networks to scale-up neuromorphic algorithms, and it is also a vital component to support within network encoding and decoding capabilities. We would like to address these areas as part of our future work.

The virtual neuron can be viewed as a tool that enables bit-level precision as well as variable precision on neuromorphic computers. We also expect the virtual neuron to be used in neuromorphic compilers that can compile high-level neuromorphic algorithms down to neurons and synapses, which can be deployed onto neuromorphic hardware directly. Another potential use case of the virtual neuron is to encode and perform operations on extremely large numbers (containing thousands of bits), as required in many cryptography applications. The virtual neuron would enable us to perform these large number operations in an energy efficient manner on neuromorphic computers. In an edge computing scenario, current neuromorphic computers allow us to perform machine learning tasks using spiking neural networks in an energy-efficient manner. However, if an application requires performing general-purpose operations on data (for instance, pre- or post-processing of data using arithmetic, logical and relational operations), we resort to conventional computers (CPUs and GPUs), which incurs significant communication cost. With approaches such as virtual neuron that serve as the building blocks of general-purpose computing on neuromorphic computers, we could potentially perform all these operations on the neuromorphic computer itself without having to communicate to the CPU/GPU and bypassing the need to transfer data back and forth from the CPU/GPU.

It is worth noting that the ultimate goal of a neuromorphic computer is *not* to perform these sorts of operations. However, many applications for which a neuromorphic system might be used (for classification, anomaly detection, control, etc.) may require these sorts of calculations as a pre- or post-processing

step for the neuromorphic system. For a continually operating neuromorphic system, for example in a control application, these sorts of calculations may be required *between* neuromorphic calculations. If these computations can take place *on* the neuromorphic computer, then it will alleviate communication costs and data movement to and from the neuromorphic system. As such, even if the computations described above are not as efficient as those on a traditional processor, it is likely that the data movement costs to and from the traditional processor will overwhelm the energy efficiency benefits gained from moving the computation back to a traditional processor.

Just like with IEEE standard data types, real numbers such as  $\sqrt{2}$ ,  $\pi$  and  $e$  cannot be directly encoded without infinite bits of precision. Therefore the bits of precision used in the virtual neuron encoding can be chosen based on the accuracy of the approximation of the real number required. Lastly, the applications demonstrated in Section VII might seem simple, but they are critical building blocks for any general-purpose computations that can be performed on a neuromorphic computer. Complex general-purpose compute tasks can be broken down into the simplest of operations defined by these functions. We would like to reiterate that the goal of this paper was to present the idea of the virtual neuron and demonstrate its performance on physical and simulated neuromorphic hardware. The demonstration on the applications mentioned in Section VII is to give the reader an idea of how the virtual neuron can be used.

### IX. CONCLUSION

Neuromorphic computing is an extremely promising paradigm for energy efficient computing in the future. It holds tremendous promise to drastically reduce the carbon footprint of computing. While traditional applications of neuromorphic computing primarily relied on SNN-based machine learning, more recent applications in graph algorithms, autonomous racing and linear algebra show that neuromorphic computing might be capable of much more than just SNNs. Neuromorphic computing has shown to be Turing-complete, and thus, capable of all general-purpose computation. A key step to realize the full potential of general-purpose neuromorphic computing is to devise effective mechanisms of encoding numbers. The current mechanisms for encoding numbers on neuromorphic computers are limited to Boolean numbers or natural numbers. But even these mechanisms are limited to the specific applications for which they were developed, and are not suitable for general-purpose computation. Moreover, some of these methods result in loss of data due to excessive discretization and/or do not preserve addition.

In this work, we presented the virtual neuron as a mechanism for encoding positive and negative integer and rational numbers. We implemented the virtual neuron in the NEST simulator and tested it on 8, 16 and 32 bit rational numbers. We theoretically compared the computational complexity of the virtual neuron to other neuromorphic encoding mechanisms. Next, we tested the virtual neuron on neuromorphic hardware and presented its time, space and power metrics.

Lastly, we demonstrated the usability of the virtual neuron by using it in five applications, that would be crucial for general-purpose neuromorphic computing. We were able to show that the virtual neuron is an efficient mechanism for encoding rational numbers. Furthermore, we also showed that the virtual neuron can mimic the artificial neuron with an identity activation function. In our future work, we would like to explore general-purpose neuromorphic algorithms and applications using virtual neurons.

## REFERENCES

- [1] A. Calimera, E. Macii, and M. Poncino, "The human brain project and neuromorphic computing," *Functional neurology*, vol. 28, no. 3, p. 191, 2013.
- [2] J. Grollier, D. Querlioz, K. Camsari, K. Everschor-Sitte, S. Fukami, and M. D. Stiles, "Neuromorphic spintronics," *Nature electronics*, vol. 3, no. 7, pp. 360–370, 2020.
- [3] F. Akopyan, J. Sawada, A. Cassidy, R. Alvarez-Icaza, J. Arthur, P. Merolla, N. Imam, Y. Nakamura, P. Datta, G.-J. Nam *et al.*, "Truenorth: Design and tool flow of a 65 mw 1 million neuron programmable neurosynaptic chip," *IEEE transactions on computer-aided design of integrated circuits and systems*, vol. 34, no. 10, pp. 1537–1557, 2015.
- [4] C. D. Schuman, J. P. Mitchell, J. T. Johnston, M. Parsa, B. Kay, P. Date, and R. M. Patton, "Resilience and robustness of spiking neural networks for neuromorphic systems," in *2020 International Joint Conference on Neural Networks (IJCNN)*. IEEE, 2020, pp. 1–10.
- [5] C. D. Schuman, S. R. Kulkarni, M. Parsa, J. P. Mitchell, B. Kay *et al.*, "Opportunities for neuromorphic computing algorithms and applications," *Nature Computational Science*, vol. 2, no. 1, pp. 10–19, 2022.
- [6] S. Ghosh-Dastidar and H. Adeli, "Spiking neural networks," *International journal of neural systems*, vol. 19, no. 04, pp. 295–308, 2009.
- [7] B. Kay, P. Date, and C. Schuman, "Neuromorphic graph algorithms: Extracting longest shortest paths and minimum spanning trees," in *Proceedings of the Neuro-inspired Computational Elements Workshop*, 2020, pp. 1–6.
- [8] C. D. Schuman, B. Kay, P. Date, R. Kannan, P. Sao, and T. E. Potok, "Sparse binary matrix-vector multiplication on neuromorphic computers," in *2021 IEEE International Parallel and Distributed Processing Symposium Workshops (IPDPSW)*. IEEE, 2021, pp. 308–311.
- [9] K. Hamilton, P. Date, B. Kay, and C. Schuman D, "Modeling epidemic spread with spike-based models," in *International Conference on Neuromorphic Systems 2020*, 2020, pp. 1–5.
- [10] P. Date, C. Schuman, B. Kay, T. Potok *et al.*, "Neuromorphic computing is Turing-complete," *arXiv preprint arXiv:2104.13983*, 2021.
- [11] P. K. Huynh, M. L. Varshika, A. Paul, M. Isik, A. Balaji, and A. Das, "Implementing spiking neural networks on neuromorphic architectures: A review," *arXiv preprint arXiv:2202.08897*, 2022.
- [12] Y. Kang and J. Chung, "A dynamic fixed-point representation for neuromorphic computing systems," in *2017 International SoC Design Conference (ISOCC)*. IEEE, 2017, pp. 44–45.
- [13] C. D. Schuman, J. S. Plank, G. Bruer, and J. Anantharaj, "Non-traditional input encoding schemes for spiking neuromorphic systems," in *2019 International Joint Conference on Neural Networks (IJCNN)*. IEEE, 2019, pp. 1–10.
- [14] M.-O. Gewaltig and M. Diesmann, "Nest (neural simulation tool)," *Scholarpedia*, vol. 2, no. 4, p. 1430, 2007.
- [15] C. Mead, "Neuromorphic electronic systems," *Proceedings of the IEEE*, vol. 78, no. 10, pp. 1629–1636, 1990.
- [16] T. Serre and T. Poggio, "A neuromorphic approach to computer vision," *Communications of the ACM*, vol. 53, no. 10, pp. 54–61, 2010.
- [17] S. H. Sung, T. J. Kim, H. Shin, H. Namkung, T. H. Im, H. S. Wang, and K. J. Lee, "Memory-centric neuromorphic computing for unstructured data processing," *Nano Research*, vol. 14, no. 9, pp. 3126–3142, 2021.
- [18] P. Blouw and C. Eliasmith, "Event-driven signal processing with neuromorphic computing systems," in *ICASSP 2020-2020 IEEE International Conference on Acoustics, Speech and Signal Processing (ICASSP)*. IEEE, 2020, pp. 8534–8538.
- [19] S. Liu and Y. Yi, "Quantized neural networks and neuromorphic computing for embedded systems," in *Intelligent System and Computing*. IntechOpen, 2020.
- [20] E. Covi, E. Donati, X. Liang, D. Kappel, H. Heidari, M. Payvand, and W. Wang, "Adaptive extreme edge computing for wearable devices," *Frontiers in Neuroscience*, vol. 15, 2021.
- [21] A. Fayyazi, M. Ansari, M. Kamal, A. Afzali-Kusha, and M. Pedram, "An ultra low-power memristive neuromorphic circuit for internet of things smart sensors," *IEEE Internet of Things Journal*, vol. 5, no. 2, pp. 1011–1022, 2018.
- [22] A. Tavanaei, M. Ghodrati, S. R. Kheradpisheh, T. Masquelier, and A. Maida, "Deep learning in spiking neural networks," *Neural networks*, vol. 111, pp. 47–63, 2019.
- [23] P. Date, *Combinatorial neural network training algorithm for neuromorphic computing*. Rensselaer Polytechnic Institute, 2019.
- [24] J. H. Lee, T. Delbruck, and M. Pfeiffer, "Training deep spiking neural networks using backpropagation," *Frontiers in neuroscience*, vol. 10, p. 508, 2016.
- [25] A. Mohemmed, S. Schliebs, S. Matsuda, and N. Kasabov, "Training spiking neural networks to associate spatio-temporal input-output spike patterns," *Neurocomputing*, vol. 107, pp. 3–10, 2013.
- [26] G. Indiveri, "Introducing 'neuromorphic computing and engineering'," *Neuromorphic Computing and Engineering*, vol. 1, no. 1, p. 010401, 2021.
- [27] A. N. Burkitt, "A review of the integrate-and-fire neuron model: I. homogeneous synaptic input," *Biological cybernetics*, vol. 95, no. 1, pp. 1–19, 2006.
- [28] B. Kay, C. Schuman, J. O'Connor, P. Date, and T. Potok, "Neuromorphic graph algorithms: Cycle detection, odd cycle detection, and max flow," in *International Conference on Neuromorphic Systems 2021*, 2021, pp. 1–7.
- [29] K. Hamilton, T. Mintz, P. Date, and C. D. Schuman, "Spike-based graph centrality measures," in *International Conference on Neuromorphic Systems 2020*, 2020, pp. 1–8.
- [30] R. Patton, C. Schuman, S. Kulkarni, M. Parsa, J. P. Mitchell, N. Q. Haas, C. Stahl, S. Paulissen, P. Date, T. Potok *et al.*, "Neuromorphic computing for autonomous racing," in *International Conference on Neuromorphic Systems 2021*, 2021, pp. 1–5.
- [31] P. Date, C. D. Carothers, J. A. Hendler, and M. Magdon-Ismael, "Efficient classification of supercomputer failures using neuromorphic computing," in *2018 IEEE Symposium Series on Computational Intelligence (SSCI)*. IEEE, 2018, pp. 242–249.
- [32] P. Date, B. Kay, C. Schuman, R. Patton, and T. Potok, "Computational complexity of neuromorphic algorithms," in *International Conference on Neuromorphic Systems 2021*, 2021, pp. 1–7.
- [33] T. Y. Choi, P. A. Merolla, J. V. Arthur, K. A. Boahen, and B. E. Shi, "Neuromorphic implementation of orientation hypercolumns," *IEEE Transactions on Circuits and Systems I: Regular Papers*, vol. 52, no. 6, pp. 1049–1060, 2005.
- [34] G. K. Cohen, G. Orchard, S.-H. Leng, J. Tapson, R. B. Benosman, and A. van Schaik, "Skimming digits: Neuromorphic classification of spike-encoded images," *Frontiers in Neuroscience*, vol. 10, 2016. [Online]. Available: <https://www.frontiersin.org/article/10.3389/fnins.2016.00184>
- [35] M. Hejda, J. Robertson, J. Bueno, J. A. Alanis, and A. Hurtado, "Neuromorphic encoding of image pixel data into rate-coded optical spike trains with a photonic vcsel-neuron," *APL Photonics*, vol. 6, no. 6, p. 060802, 2021. [Online]. Available: <https://doi.org/10.1063/1.50048674>
- [36] A. Sengupta and K. Roy, "Encoding neural and synaptic functionalities in electron spin: A pathway to efficient neuromorphic computing," *Applied Physics Reviews*, vol. 4, no. 4, p. 041105, 2017. [Online]. Available: <https://doi.org/10.1063/1.5012763>
- [37] Y. Yi, Y. Liao, B. Wang, X. Fu, F. Shen, H. Hou, and L. Liu, "Fpga based spike-time dependent encoder and reservoir design in neuromorphic computing processors," *Microprocessors and Microsystems*, vol. 46, pp. 175–183, 2016. [Online]. Available: <https://www.sciencedirect.com/science/article/pii/S0141933116300060>
- [38] O. Iaroshenko and A. T. Sornborger, "Binary operations on neuromorphic hardware with application to linear algebraic operations and stochastic equations," 2021. [Online]. Available: <https://arxiv.org/abs/2103.09198>
- [39] S. Lawrence, A. Yandapalli, and S. Rao, "Matrix multiplication by neuromorphic computing," *Neurocomputing*, vol. 431, pp. 179–187, 2021. [Online]. Available: <https://www.sciencedirect.com/science/article/pii/S0925231220316416>
- [40] C. Zhao, W. Danesh, B. T. Wysocki, and Y. Yi, "Neuromorphic encoding system design with chaos based cmos analog neuron," in *2015 IEEE*

*Symposium on Computational Intelligence for Security and Defense Applications (CISDA)*, 2015, pp. 1–6.

- [41] C. Zhao, B. T. Wysocki, Y. Liu, C. D. Thiem, N. R. McDonald, and Y. Yi, “Spike-time-dependent encoding for neuromorphic processors,” *J. Emerg. Technol. Comput. Syst.*, vol. 12, no. 3, sep 2015. [Online]. Available: <https://doi.org/10.1145/2738040>
- [42] C. Zhao, J. Li, and Y. Yi, “Making neural encoding robust and energy efficient: An advanced analog temporal encoder for brain-inspired computing systems,” in *Proceedings of the 35th International Conference on Computer-Aided Design*, ser. ICCAD ’16. New York, NY, USA: Association for Computing Machinery, 2016. [Online]. Available: <https://doi.org/10.1145/2966986.2967052>
- [43] Z. Wang, X. Gu, R. Goh, J. T. Zhou, and T. Luo, “Efficient spiking neural networks with radix encoding,” *arXiv preprint arXiv:2105.06943*, 2021.
- [44] J. Plank, C. Zheng, C. Schuman, and C. Dean, “Spiking neuromorphic networks for binary tasks,” in *International Conference on Neuromorphic Systems 2021*, 2021, pp. 1–9.
- [45] A. M. George, R. Sharma, and S. Rao, “Ieee 754 floating-point addition for neuromorphic architecture,” vol. 366, pp. 74–85. [Online]. Available: <https://www.sciencedirect.com/science/article/pii/S0925231219308884>
- [46] K. Dubey, U. Kothari, and S. Rao, “Floating-point multiplication using neuromorphic computing.” [Online]. Available: <https://arxiv.org/abs/2008.13245>
- [47] J. P. Mitchell, C. D. Schuman, R. M. Patton, and T. E. Potok, “Caspian: A neuromorphic development platform,” in *Proceedings of the Neuro-Inspired Computational Elements Workshop*, ser. NICE ’20. New York, NY, USA: Association for Computing Machinery. [Online]. Available: <https://doi.org/10.1145/3381755.3381764>
- [48] G. Chakma, N. D. Skuda, C. D. Schuman, J. S. Plank, M. E. Dean, and G. S. Rose, “Energy and area efficiency in neuromorphic computing for resource constrained devices,” in *Proceedings of ACM Great Lake Symposium on VLSI (GLSVLSI)*, pp. 379–383.